# A highly stable and efficient spherical underwater robot with hybrid propulsion devices

Shuoxin Gu[1,2] · Shuxiang Guo[1,3] · Liang Zheng[1]

## Abstract

Underwater robots have been promoted a significant interest in monitoring the marine environment. In some complex situation, robots sometimes need to keep moving fast, sometimes need to keep low speed and low noise. To address this issue, a novel spherical underwater robot (SUR IV) with hybrid propulsion devices including vectored water-jet and propeller thrusters is proposed in this paper. The diversity of the movement modes is also proposed for the different targets as remote or hover and general or silent. To analyze the hydrodynamic characteristics of the hybrid thruster, the computational fluid dynamics simulation is calculated in ANSYS CFX by using the multi-reference frame method. The simulation results show the interaction between the propeller and water-jet thruster. The thrust experiment to evaluate the performance of the improved hybrid thruster is also conducted. The maximum thrust of the hybrid thruster is increased 2.27 times than before. In addition, a noise comparison experiment is conducted to verify the low noise of the water-jet thruster. Finally, the 3 DoF motions which include the surge, heave and yaw for the SUR IV were carried out in the swimming pool. The improvement of the overall robot is assessed by the experimental results.

## 1 Introduction

The exploration and discovery in the unknown ocean are developed more and more quickly, the autonomous underwater vehicles (AUVs) are widely used in oceanographic research (Russell et al. 2014; Mai et al. 2016). Different

✉ Shuxiang Guo
guo@eng.kagawa-u.ac.jp

Shuoxin Gu
gsx@cuit.edu.cn

Liang Zheng
s18d505@stu.kagawa-u.ac.jp

[1] Faculty of Engineering, Kagawa University, Takamatsu, Kagawa, Japan

[2] School of Control Engineering, Chengdu University of Information Technology, Chengdu, Sichuan, China

[3] Key Laboratory of Convergence Medical Engineering System and Healthcare Technology, The Ministry of Industry and Information Technology, School of Life Science and Technology, Beijing Institute of Technology, Beijing, China

configurations, shapes and propulsion methods for underwater vehicles are corresponded to different applications. For example, a smaller, flexible and low-speed design of the robot may be reasonable for underwater applications so as to easily enter some small places (Bhattacharyya et al. 2016). The spherical shape also employs in an amphibious robot which can both walk on land and swim under water (Li et al. 2016; Zheng et al. 2018). The streamlined shape is required for high-speed movements (Hanff et al. 2017). The flow field numerical simulation of an underwater vehicle with streamlined shape was carried out in (Dong et al. 2012). As we all know, the propulsion device employs an important role in controlling the movement of the underwater robot. There are various designs for propulsion device, such as propellers, poles, magneto hydrodynamic drives and bionic propulsion device (Claus et al. 2012; Zhou et al. 2017). Especially, the propeller is the most common propulsion method for underwater vehicles. Chen et al. (2016) proposed a foldable propeller for a hybrid-driven underwater glider. A reconfigurable magnetic coupling thruster is designed and developed by researchers in Laboratoire Brestois de Mécaniques et des Systèmes. Based on the radial magnetic coupling as

the joint, the vectorial propeller thruster can rotate and not contact directly with the motor (Chocron et al. 2014; Vega et al. 2016; Gasparoto et al. 2017). Not only that, but the propeller also can be applied in biomimetic underwater robots (Pan et al. 2011; Gao et al. 2011; Scaradozzi et al. 2017). A novel type of spherical underwater robot that uses only a single pump and two fluidic valves to achieve three dimensional motions is proposed by (Mazumdar et al. 2013). Lv et al. (2014) developed a type of distributed pump-jet propulsion system (DPJP) with two or four specially designed pump-jet pods located around the axisymmetric underwater vehicle body symmetrically. For documentation purposes, a biomimetic research autonomous vehicle is presented which consists of two different types of thrusters (Scaradozzi et al. 2017). Researchers in the Tall University of Technology presents a biomimetic underwater robot U-CAT with a novel 4-fin actuation (Salumäe et al. 2014). (Georgiades et al. 2004) describes an underwater walking robotic system which allows to navigate and map clear shallower-water.

In our previous research, a spherical underwater robot equipped with multiple vectored water jet-based thrusts was proposed and designed (Lin and Guo 2012; Lin et al. 2013). On this basis, (Yue et al. 2015a) described the development of the second-generation Spherical Underwater Robot (SUR-II). The hydrodynamic analysis was carried out to verify the estimated parameters such as the velocity vectors, pressure contours and drag coefficient (Yue et al. 2013). In the follow-up study, a father-son underwater intervention robotic system was proposed to realize the underwater manipulation for the narrow space exploration (Yue et al. 2015b). The next development of the SUR was that (Li et al. 2015; Li and Guo 2016) proposed the third-generation spherical underwater robot (SUR III) with four water-jet thrusters. And the acoustic communication methods were also proposed for SUR III (Li et al. 2017). Then (Gu and Guo 2017) proposed the research of the performance evaluation of the SUR III in the static mechanical and hydrodynamic analysis. Based on the previous view (Gu et al. 2017), proposed a hybrid propulsion device for the SUR III. However, few designs have taken a hybrid propulsion device on an underwater robot into consideration. The device can provide advantages such as keeping stability and accuracy to the specific location with the low-speed mode, improving velocity to a certain area with the high-speed mode. On the downside, the low-speed mode robot will waste a lot of time for long distance navigation, and high-speed robot close to the object with a lot of noise and can't guarantee the accuracy of position. Therefore, it is extremely important for underwater robots to provide a hybrid propulsion mode of high and low speed, as well as keep quiet in low speed mode during ocean inspections.

In this paper, a novel spherical underwater robot with hybrid propulsion device was proposed in Sect. 2. This kind of high and low speed hybrid propulsion mode can not only save the detection time and improve the work efficiency, but also can improve the detection precision and accuracy when slowly approaching the target. The hydrodynamic analysis of the propeller was presented to explain how a propeller generates thrust in Sect. 3. The CFD simulation is carried out to calculate the hydrodynamic characteristic for the propeller. Experiments of different propulsion mode at the different voltage in negative and positive rotation are conducted to verify the better performance of the hybrid thruster in Sect. 4. Experiments in the pool were carried out to evaluate the underwater performance for the robot in Sect. 4. Then a further discussion about the scope and limitation of the proposed system is discussed in Sect. 5. Finally, conclusions are drawn in Sect. 6.

## 2 Spherical hybrid-thrust robot design

### 2.1 Previous research of the spherical underwater robot

In our previous research, a spherical underwater robot was proposed with multi vectored water-jet thrusters. The first and second-generation spherical underwater robots both owned three vectored water-jet thrusters which are evenly distributed around the shell of the robot. In order to enhance the power management, the third-generation spherical underwater robot (SUR III) was developed with four vectored water-jet thrusters symmetrically distributed. The configuration and dimensions of these spherical underwater robots are illustrated in Fig. 1. Figure 1b displays the overall view of the previous SUR III.

In general, the underwater robot has 6 Degrees of Freedom (DoF) which include surge, sway, heave, roll, pitch and yaw. According to the different DoF for an underwater robot (Yue et al. 2015a, b). In different research of the attitude and motion for the underwater robot, DoF as sway, roll and pitch are rarely used underwater, but in the optical documentational surveys the roll and pitch correction are important, such as the research (Drap et al. 2007, 2008) mentioned. Table 1 reveals the utilization ratios of motion. In previous research, the SUR III can be realized four DoF which involve surge, sway, heave and yaw. These DoF which are also illustrated in Fig. 1b can satisfy the robot to move freely in the water.

The novel propulsion system not only needs to retain these DoF, but also needs to increase the propulsive force.

Figure 2 illustrates the structure of the previous vectored water-jet thruster for the SUR III. There are two servo motors, one DC motor, and some support parts in one set of the thruster. It also has already verified that the structure is stable and reliable for SUR III (Gu and Guo 2017; Gu et al. 2017).

**Fig. 1** Overall view of the spherical underwater robots



**(a)** The 3D model of the SUR II          **(b)** The 3D model of the SUR III
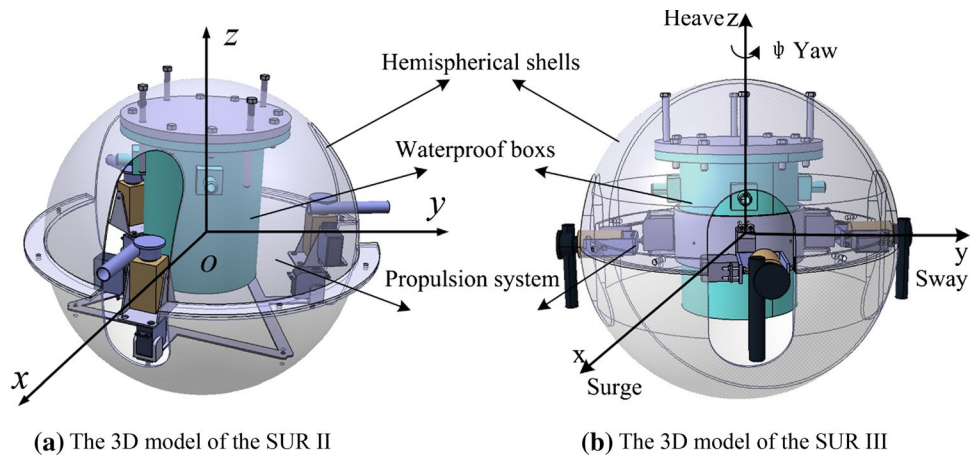
**Table 1** Utilization ratio of different DoF

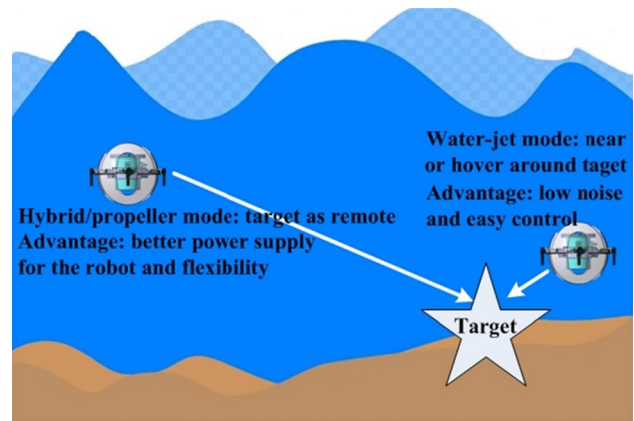| DoF | Surge | Sway | Heave | Roll | Pitch | Yaw |
|---|---|---|---|---|---|---|
| Utilization ratio | 100% | 31% | 96% | 33% | 7% | 100% |
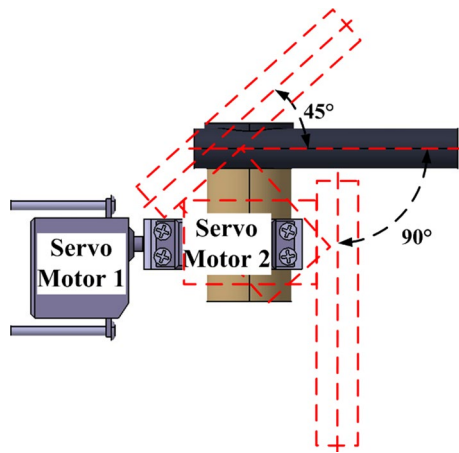


**Fig. 2** The vectored water-jet thruster of the SUR III



**Fig. 3** Advantages of the hybrid modes

## 2.2 Conceptual and mechanical design of the hybrid propulsion device

The propeller is often employed as the thruster in the propulsion device for the underwater robot. Its good power management and reliability are all we need. However, the noise of the propeller is higher than the water-jet thruster. Therefore, a hybrid propulsion device which includes both the water-jet and propeller thruster is proposed to improve the hydrodynamic thrust of the SUR IV in the restricted space and structure. In the underwater mission as shown in Fig. 3, alternative methods of the hybrid and propeller propulsion mode can quickly and effectively close to the target, then switch the water-jet propulsion mode to reduce the noise near the target.

A better improvement of the thruster needs not to affect the movements of the robot while ensuring the increase of the power management, thus, a novel type of hybrid thruster is born as shown in Fig. 4. The structure diagram in Fig. 4a displays the details of the hybrid thruster including one servo motor, one propeller, one water-jet thruster, supports and the servo arm which are employed to connect the servo motor and DC motors. From the side view of the hybrid thruster in Fig. 4b, the propeller and water-jet thruster will rotate together from 0°to 180°. The combination of these movement changes is enough to achieve the basic motion of the SUR IV. The sealed box shown in Fig. 5 is printed by the 3D printer for all DC motors and the silicone gel is used for filling the gaps of the box as a base seal. The 3D model of the SUR IV is shown in Fig. 6. The max diameter of the spherical shell is 46 cm and the distance between two opposite thrusters is 52 cm.
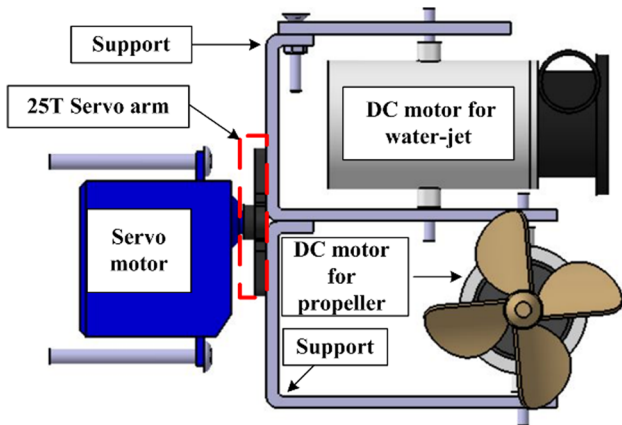
**(a)** The structure diagram of the hybrid thruster
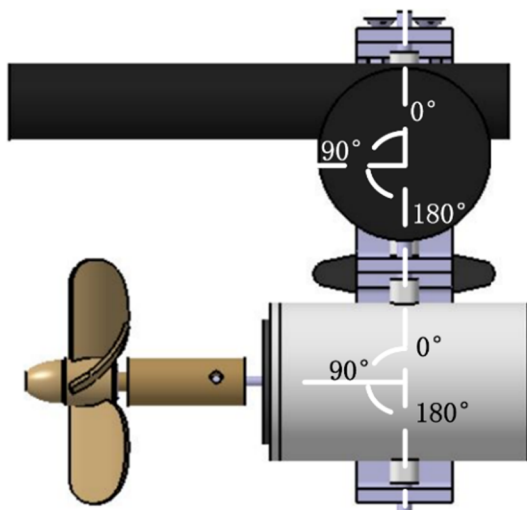


**(b)** Side view of the hybrid thruster

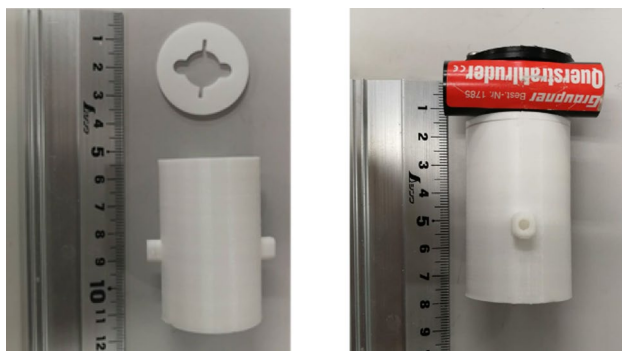**Fig. 4** The improved hybrid thruster



**Fig. 5** Seal design of the dynamical thruster

## 2.3 Motion state of SUR IV

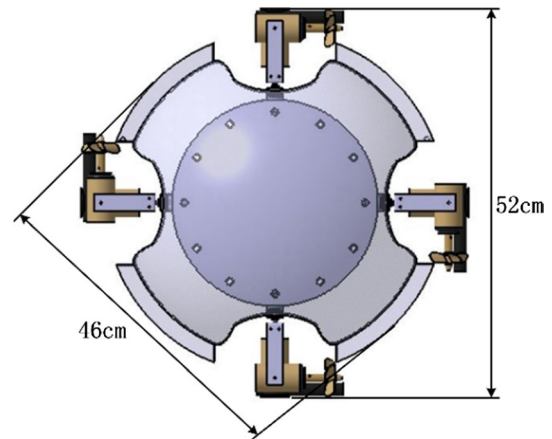There are still four DOF which included surge, sway, heave and yaw of the novel SUR. From the Fig. 2b we know that



**Fig. 6** The 3D model of SUR IV



**(a)** High-speed forward motion      **(b)** Rotation motion

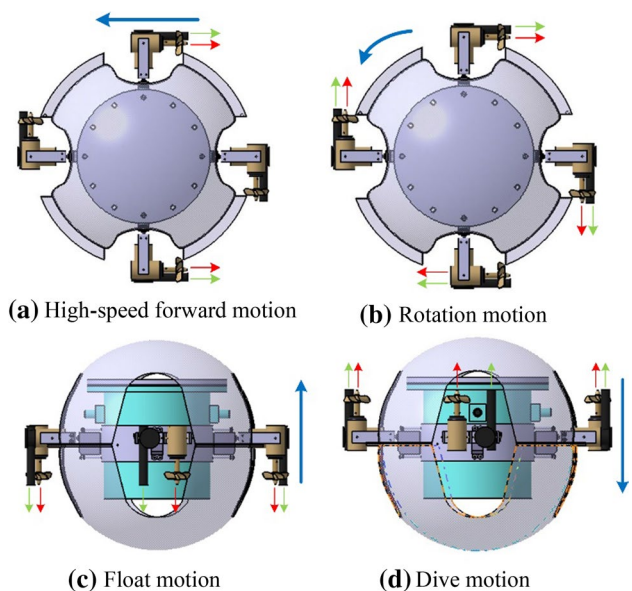**(c)** Float motion      **(d)** Dive motion

**Fig. 7** Motion state of the SUR IV

the DoF of the surge and sway are the movement in the same plane. Thus, three DOF which are surge, heave and yaw are focused in this paper. In surge motion, two opposite hybrid thrusters are regarded as water-jet, propeller and hybrid mode by switching working conditions of the propeller and water-jet thrusters. The Fig. 7a shows the high-speed forward motion of the SUR IV. At this point, propeller and water-jet work together to generate thrust for the robot. The rotation motion is shown in Fig. 7b, although the rotation angle of the servo motor is limited, the reversal of the DC motor can make up for this shortcoming. In yaw motion, the rotation angle can be measured by the 6 DoF inertial sensor. If all thrusters work at the same time, the robot can be realized a high-speed rotating mode which is shown in Fig. 7b, this style is suitable for fast turning requirement. Otherwise

working of two opposite vectored propeller thrusters or four vectored water-jet thrusters will realize a low-speed rotating mode. Due to the low speed with water-jet mode, it is easier to change the states of the robot with shorter braking time or braking angles and switch to a low-noise mode. The final one is the heave motion which involved two kinds of motion: dive and float motions, corresponding to Fig. 7c, d. The positive and negative rotation of DC motors can switch these two motions without the operation of servo motors.

## 2.4 Control circuit

In order to allow the SUR IV to switch between three propulsion modes depending on the environment, the control circuit is designed as shown in Fig. 8. The ATMega2560 is employed as the control center. Although achieve 4 DoF movements. For the heave motion, it is the quantity of servo motors is reduced, the use of the positive and negative rotation of the DC motor can still possible to switch the dive and float motion by using the positive and negative rotation of the DC motor even without the operation of servo motors. The H-Bridge MOSFETs control boards are used to receive the PWM signals for the propeller thruster speed regulation and positive/negative rotation. Taking into account the low thrust and insufficient PWM ports, the H-Bridge relay is used to control the negative and positive rotation of the water-jet thruster without speed regulation. The application of different sensors will achieve the closed-loop control system. Sensors which can provide feedbacks underwater are also employed in the SUR IV. The servo motors and DC motors can adjust the robot's attitude in time to feedbacks. The depth sensor is ADPW11 from Panasonic which can measure a depth of 7 m. The 6-DoF inertial sensor is
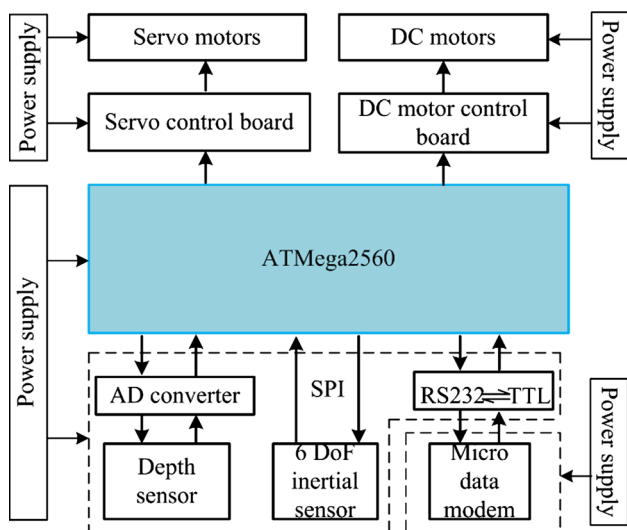
ADIS16365 from analog device. Finally, the acoustic communication module is Micron data modem from Tritech.

# 3 Hybrid thruster simulation and verification

## 3.1 CFD simulation and results

The 3D model of the hybrid thruster is established in CATIA. And the parameters of the propeller and water-jet thruster are given in Table 2. Based on the multi-reference frame method, the geometry included the station and rotation domain are created in CFX which belongs to the ANSYS WORKBENCH. Both of the station domain and rotation domain for propeller are assumed as the cylinder in this simulation. Figure 9a illustrates the overall plot of the fluid module. The length and diameter of the cylinder can define the boundary of the domains. The propeller rotation domain boundary is $0.5D_1$ for length and $1.2D_1$ for diameter, and the station domain is $10D_1$ for length and $8D_1$ for diameter. Figure 9b illustrates the simplified hybrid thruster in the rotation domain. The distance between the center of the propeller and water-jet is 6.2 cm which is corresponding to the actual assembly situation. Then mesh is also the indispensable step of the CFD simulation. The mesh is generated by using the hex-dominant method. This method is often used for geometries that cannot be swept and can generate unstructured hexahedral domain meshes with a small number of pyramidal and tetrahedral elements. In this CFD simulation, the intumescent layer, off-axis and quadrature mass within an acceptable range are not required, so the hex-dominant method is suitable. The inlet velocity of the station domain is 0.2 m/s. The speed of the rotation domain is the same as the maximum speed of the propeller and set to 400 rev/min. The station domain is the turbulence handled by the k–ε model. The environment condition is set as the isothermal temperature of 20 °C. Before start calculating, the convergence criterion is set as $1 \times 10^{-5}$ in the solver control. According to the results shown convergence in the CFX post-processing, the vector and streamline of the velocity is shown in Fig. 10. The streamlines of the propeller and water-jet show the path of 150 particles in the flowing fluid



**Fig. 8** The control circuit of the SUR IV

**Table 2** Parameters of the propeller

| Item | List of items | Value |
|---|---|---|
| Propeller | Diameter of the propeller, $D_1$ | 50 mm |
| | Hub/propeller diameter ratio, dh/D | 0.2 |
| | Number of blades, Nb | 4 |
| Water-jet thruster | Nozzle diameter, $D_2$ | 14 mm |
| | Blade diameter, $D_3$ | 23 mm |

**Fig. 9** Overall plot of the fluid model



**(a)** The flow field module

**(b)** The rotation domain



**(a)** Velocity streamline
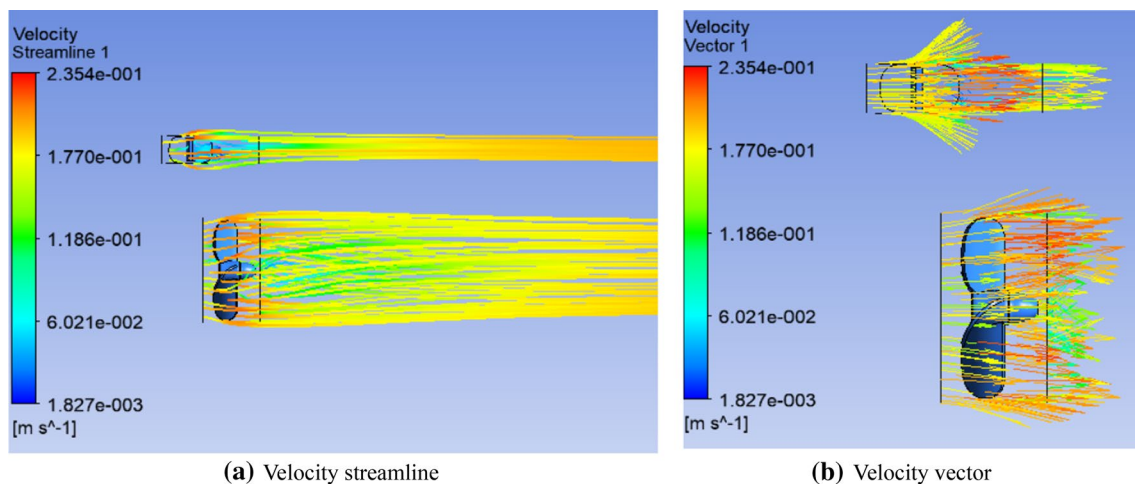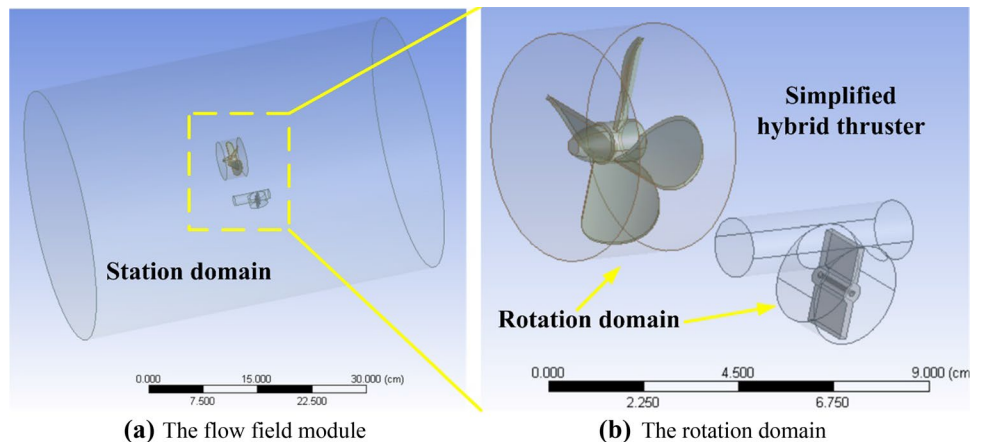
**(b)** Velocity vector

**Fig. 10** Vector and streamline of the velocity

respectively. It can be seen that at the current distance, the interaction between the two thrusters can be ignored.

### 3.2 Thrust experiments and results of the hybrid thruster

In Fig. 11, the thrust experimental setup consists of a 6-DoF load cell, a hybrid thruster with water-jet and propeller, a servo motor and some rigid connection bars. The coordinate system of the experimental setup can refer to Fig. 11b. For the reason to better evaluate its performance, the experiments are divided into 6 cases that include the positive and negative rotation of the water-jet, propeller and hybrid mode. For each case, the thrust at different voltage is also measured. The rated voltage of the DC motor is 7.2 V, so the maximum voltage of this experiment is set as 7 V.
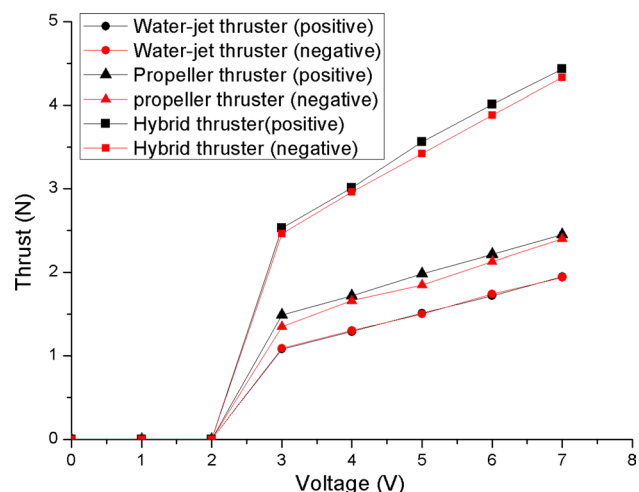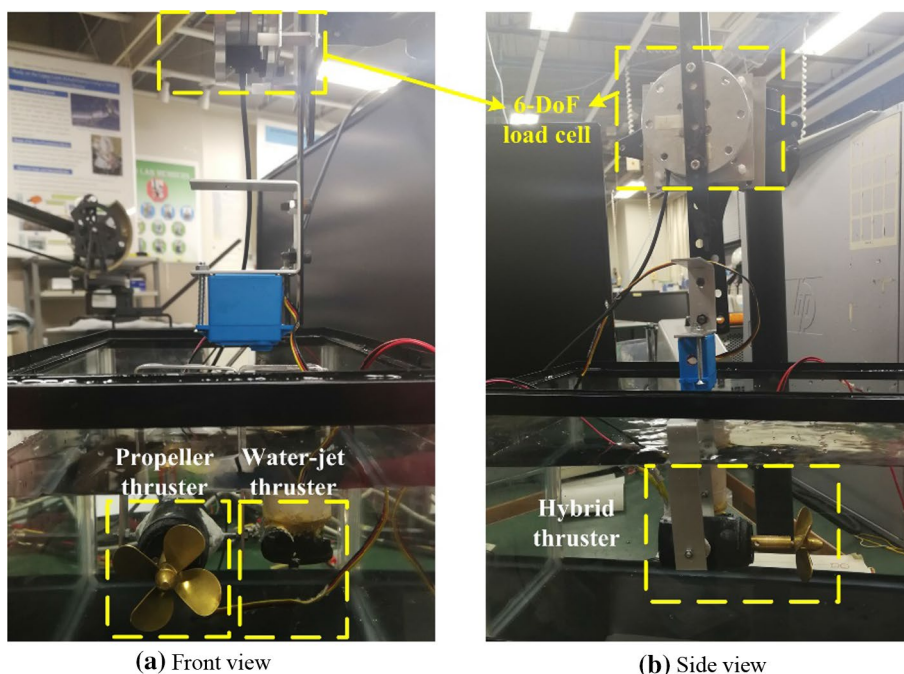
The experimental results are summarized in Fig. 12. The DC motor will start at the voltage above 3 V. For the water-jet thruster mode, the positive and negative rotation of the blade will not affect the thrust. For the propeller thruster,

the thrust of the negative rotation is slightly smaller than the positive rotation. The difference of these two cases is 2% at 7 V and can be ignored. The maximum thrust of the propeller at 7 V is 2.45 N and it is 22.5% stronger than the water-jet-thruster at the same condition. Finally, for the hybrid mode, the interaction between the water-jet and propeller thruster is not too great from the experimental results. In the same way, the difference in positive and negative thrusts is tiny as 2.3%. The maximum thrust of the hybrid thruster at 7 V is 4.43 N and it is increased 127% stronger than the water-jet thruster and 80.8% stronger than the propeller thruster.

### 3.3 Noise comparison experiments and results

To compare the noise between the different mode, a simple comparison experiment is carried out. The hybrid thruster sets in the middle of the tank (60 cm × 30 cm × 35 cm) as shown in the Fig. 13. Four measuring points are placed on the four walls of the tank. The noise of the water-jet mode,
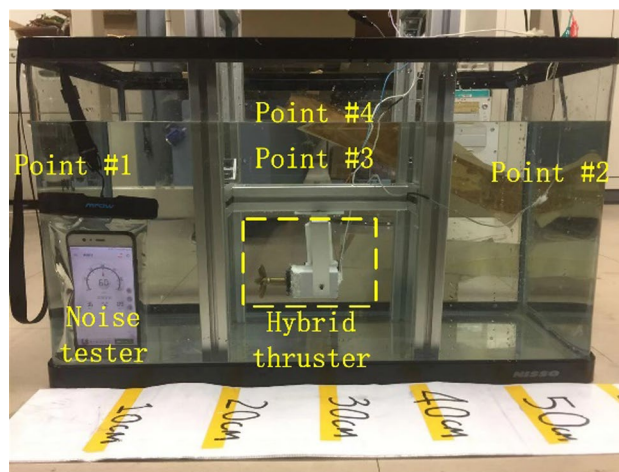
**Fig. 11** Thrust experimental setup



**(a)** Front view          **(b)** Side view



**Fig. 12** Experimental results for the different thrusters



**Fig. 13** Noisy experimental setup

propeller mode and hybrid mode are measured at every point for 10 times by using the noise tester in the cellphone.

The noise comparison experimental results are illustrated in Fig. 14. The initial noise is 56 dB. The experimental results show that the water-jet mode has the lowest noise regardless of the measuring position.

## 4 Experiments and results for basic motion

In order to evaluate the performance of the hybrid thruster and the novel robot, some experiments are carried out in this Section.

The prototype of the SUR IV is shown in Fig. 15. The underwater characteristics of the SUR IV are also the focus of this research. The underwater experiments were completed in a swimming pool with the length of 25 m, the width of 11 m and the depth of 1.1 m. The experiments are divided into the following cases: high-speed forward motion in surge, dive and float motion in heave, and rotation motion in yaw.

### 4.1 Case I: High-speed forward motion in surge

In this case, the SUR IV moved in the pool by using two opposite hybrid thrusters. The Fig. 16 shows that the motion
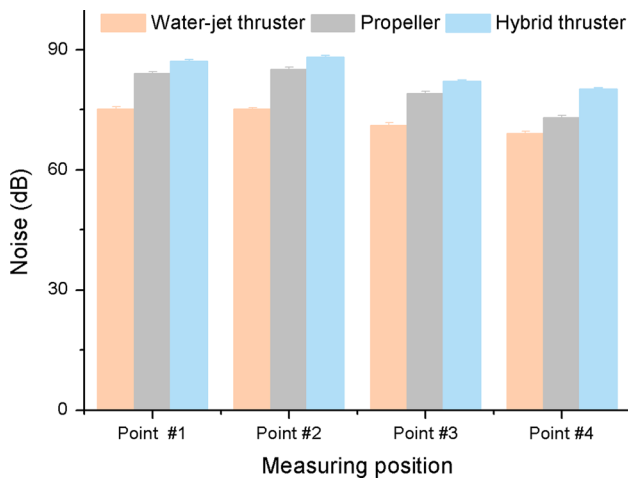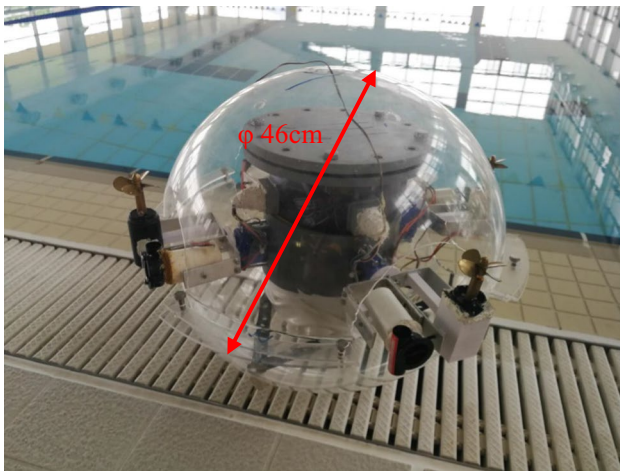
**Fig. 14** Noise comparison of thrusters



**Fig. 15** The prototype of the SUR IV

state from 0 to 20 s and the total distance of movement is 4 m. The triangle logos in Fig. 16a–e are the start point of the SUR IV.

The relationship between the distance and time of the SUR II (Lin and Guo 2012; Yue et al. 2015a, b), SUR III (Li et al. 2017) and SUR IV are shown as the blue lines in the Fig. 17. For the same time conditions, the SUR IV has a greater ability to travel long distances. The average velocity of the SUR IV can be calculated as 0.2 m/s, but at the beginning 5 s, the robot is in an accelerated state, the average velocity is less than 0.2 m/s. After 5 s, the robot enters a constant state with an average velocity more than 0.2 m/s. The green lines in the Fig. 17 illustrate the velocity comparison of the SUR II (Lin and Guo 2012; Yue et al. 2015a, b), SUR III (Li et al. 2017) and SUR IV. By comparison, the max velocity of the SUR IV is increased by 33.3% more for the forward motion than the last generation design. The 6-DoF

inertial sensor records an elevation angle between 5°–12° in pitch at the beginning of the surge motion. This may be due to the lower thrust position of the propeller, and the deflection is limited less than 8° during the remaining voyage.

### 4.2 Case II: Dive and float in heave motion

For the dive and float motion, four hybrid thrusters will work together to make the robot keep stable. In this case, the robot first dives to the bottom of the pool and then floats back to the surface. Although the buoyancy of the robot is greater than the gravity, hybrid thrusters are still employed in the float motion. In order to make the SUR IV freely dive and float underwater, the relationship between buoyancy and gravity was considered at the beginning of the design. While ensuring that the robot as a whole float on the surface of the water, the propulsion device can be left underwater. Meanwhile, in order to prevent the robot from crashing to the bottom, the pressure sensor will reserve a 20 cm bottoming pre-tip for the robot in dive motion. The experimental time-sharing process is shown in the Figs. 18 and 19. The center of the robot is set as the reference point for recording the experimental data. The initial depth of the robot for dive motion is 0.2 m. After 4 s, the SUR IV touches the pool bottom without collision as the blue line shown in Fig. 20. Influence of the buoyancy on float motion is not great as shown in Fig. 20. The average speed of the dive and float motion is almost 0.2 m/s. These results are also compared with the SUR II (Lin and Guo 2012; Yue et al. 2015a, b) and SUR III (Li et al. 2017) in Fig. 20. At the same time, the deflection of the robot in pitch and roll is small enough to be negligible in heave motion.

### 4.3 Case III: Rotation motion in yaw

For the spherical underwater robot, in situ turning is one of the major advantages for the underwater movement. That makes the robot working flexibly in small spaces without regard to the turning radius. In the previous section, the anticlockwise rotation state of the SUR IV is given in the Fig. 7b. Three of the hybrid thrusters are turning positively and the remaining one needs to be reversed. All the DC motors in the clockwise rotation are opposite to the anticlockwise. Figures 21 and 22 record the process in which the SUR IV rotates anticlockwise and clockwise by 360°. As shown, in the clockwise rotation, the SUR IV completed a 360-degree rotation in 4 s with an average speed of 90 degrees/s. The same process is completed in 3 s in anticlockwise rotation with an average speed of 120 degrees/s. The experimental results are shown in Fig. 23. The reason for this difference may be related to the difference between the positive and negative thrusts of the hybrid thruster. This reference is not obvious in the thrust experiment for the
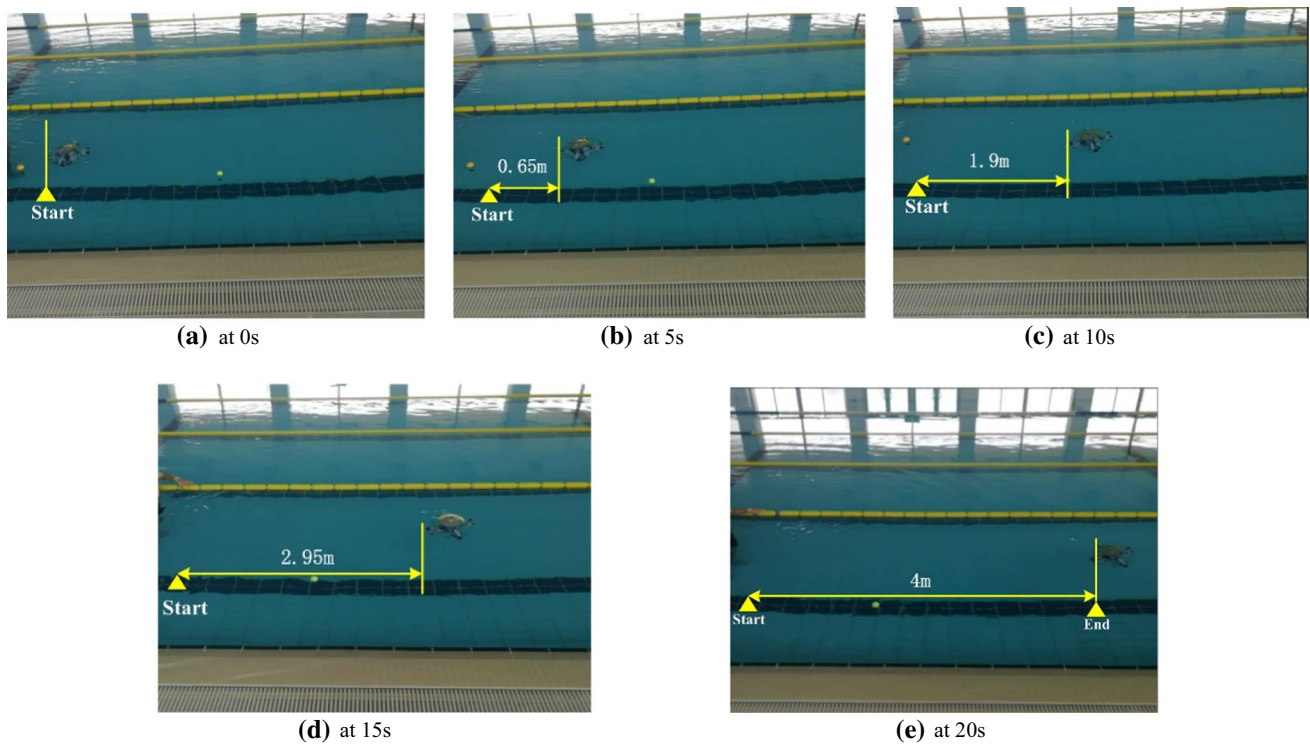
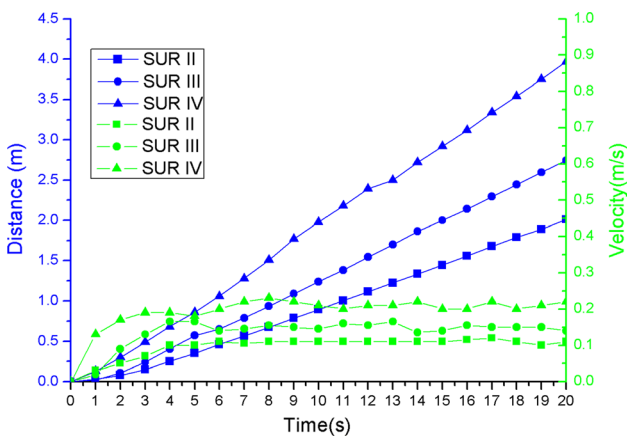**Fig. 16** High-speed forward motion in surge



**Fig. 17** Relationship between distance, velocity and time of the forward motion in surge for SUR II, SUR III and SUR IV

single hybrid thruster, but there will be obvious in the robot movement.

## 5 Discussion

Underwater robots are very helpful for underwater research and exploration in different fields. The spherical shape allows the robot to make flexible turns underwater even in the narrow spaces. Nevertheless, few designs have taken the hybrid propulsion device for remote and hover tasks into account.

In the present work, a novel spherical underwater robot with the hybrid device including both water-jet thrusters and propellers was proposed. The thrust of the thrusters can be measured by the load cell. The thrust comparison between the water-jet thruster, propeller and the hybrid thruster, shown in Fig. 12, was obtained by the experiment. The Fig. 17 showed the relationship between distance, velocity and time of the forward motion in surge for SUR II, SUR III and SUR IV, respectively. In long-distance missions, the advantages of the hybrid propulsion device are significant. The comparison of the dive and float motion in heave is illustrated in Fig. 20, although the limited depth of the pool, the effect of the buoyancy on the robot and the closed-loop feedback of the bottoming pre-tip can be observed. Despite the difference of the thrust for the single thruster in anti-clockwise and clockwise is not so large, the experimental results in Fig. 23 showed that the difference between the anticlockwise and clockwise rotation in yaw motion cannot be ignored. This provided an experimental basis for how to improve accuracy and efficiency in the actual complex task.

In the previous research, some researchers focus on the single propulsion method, such as the single jet thruster (Bhattacharyya et al. 2016) or multi water-jet thrusters (Mazumdar et al. 2013, Lin and Guo 2012, Yue et al. 2015a,
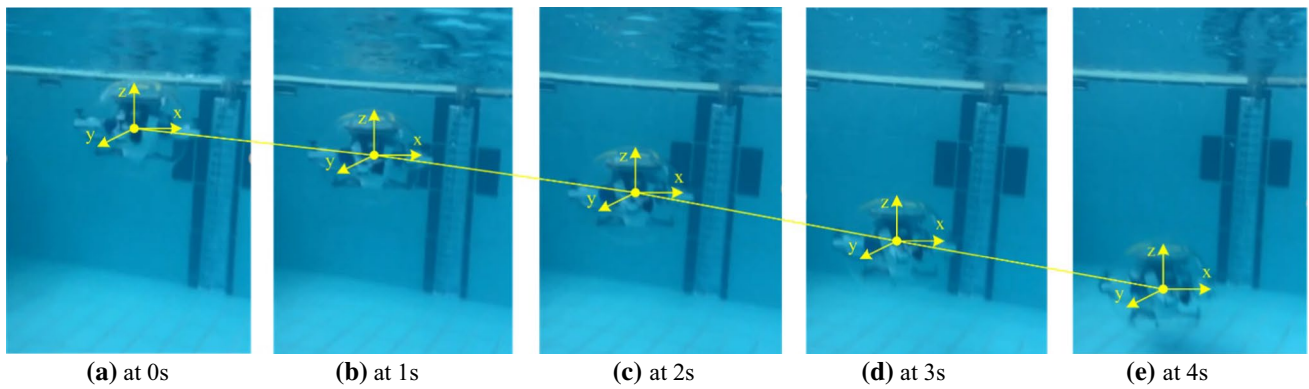
| **(a)** at 0s | **(b)** at 1s | **(c)** at 2s | **(d)** at 3s | **(e)** at 4s |

**Fig. 18** Dive motion in heave



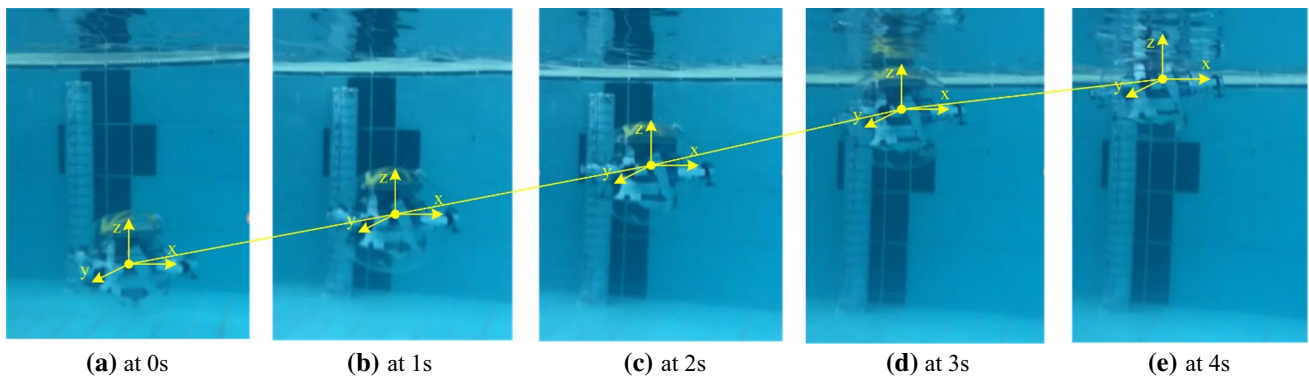| **(a)** at 0s | **(b)** at 1s | **(c)** at 2s | **(d)** at 3s | **(e)** at 4s |

**Fig. 19** Float Motion in heave
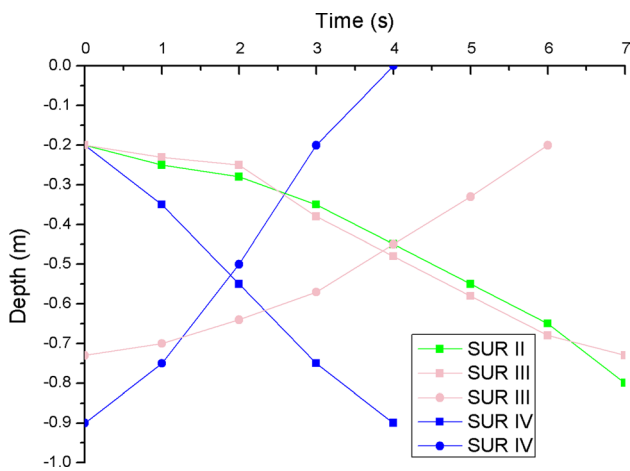


**Fig. 20** Experimental results of the dive and float motion in heave of SUR II, SUR III and SUR IV

b, Li et al. 2017), the magnetic coupling propeller thruster (Hanff et al. 2017, Chocron et al. 2014, Vega et al. 2016, Gasparoto et al. 2017) and the pump jet thruster [5]. In these studies, the reasons for using the single propulsion method are the application environment, the purpose of being *easy to*



| **(a)** at 0s | **(b)** at 1s |
| **(c)** at 2s | **(d)** at 3s |

**Fig. 21** Rotation motion (Anticlockwise) in yaw

**(a)** at 0s      **(b)** at 1s

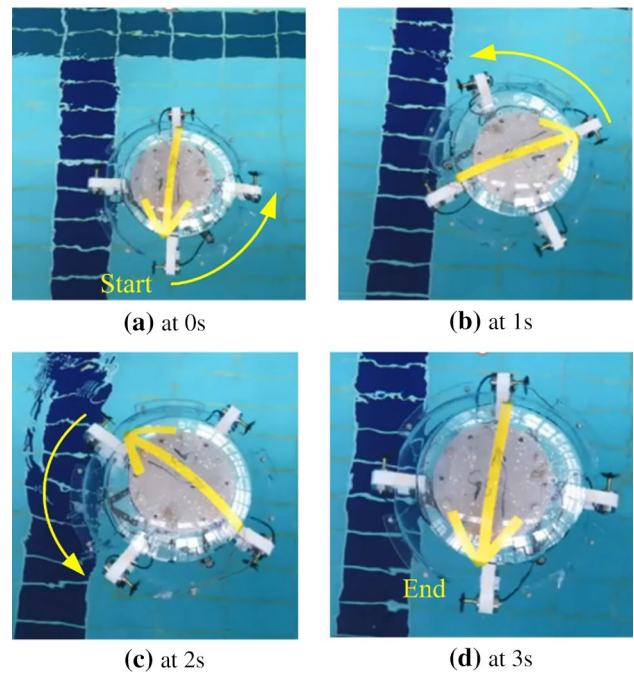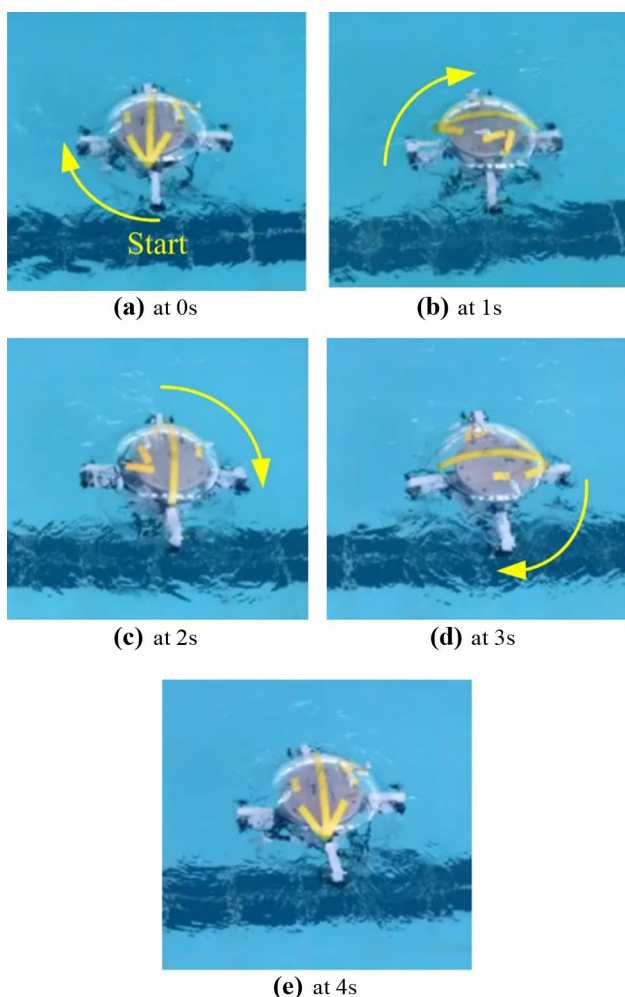**(c)** at 2s      **(d)** at 3s

**(e)** at 4s
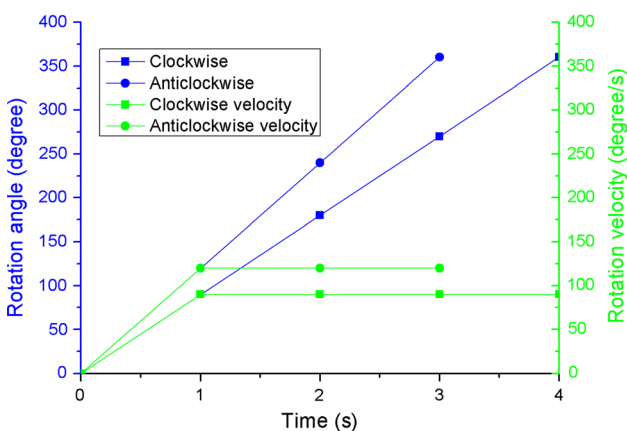
**Fig. 22** Rotation motion (Clockwise) in yaw



**Fig. 23** Experimental results of the rotation motion in yaw

waterproof or just for one or two degrees of freedom motion. Biomaterials are also often employed in underwater micro-robots. Researchers achieve the multi-degree-of-freedom of the robot by controlling the different movement mode of different parts on the robot (Pan et al. 2011). The goal of these previous studies is to establish a precise and flexible propulsion device for the robot. However, the precise and flexible propulsion device needs to adapt to multivariate underwater environments, such as distance changes and noise requirements. The proposed device in this research is capable of the long-distance mission with rapid propulsion and the close-range cruise with low-noise.

Despite the promising results, it is important to notice that the study is limited by the fact that the experiments for a single degree of freedom in the pool were carried out to conduct the performance evaluation of the SUR IV. The experiment of the single DoF motion can only reflect the performance of the robot in two dimensions, while the underwater environment is mostly three-dimensional. In addition, the depth limitation of the pool does not provide more experimental data and reference for the effects of buoyancy on the robot. And the water environment of the pool is also simple and steady. Therefore, the direction for future research is to perform experiments of the complex task planning in a wider complex three-dimensional water environment.

## 6 Conclusions

This paper presented a hybrid propulsion device for the fourth-generation spherical underwater robot (SUR IV). First of all, the novel mechanism of the hybrid-propulsion device was proposed. This novel hybrid propulsion device, including both propeller and water-jet thrusters, which can realize the fast switching between the high speed and low speed for the robot. In high speed mode, the robot can approach the target quickly. In low speed mode, the status of the robot is easier to be changed to avoid collision and noisy. At the same time, the water-jet thruster will avoid being caught by underwater plant. After that, the CFD simulation with the multi-reference frame method for the hybrid thruster was carried out. The simulation results show that there is no interference on the respective jet path in the assembly distance. Then, experiments for measuring the thrust of different cases for thrusters were conducted by using a 6-DOF load cell. The positive and negative rotation of the DC motor does not affect the thrust of both water-jet and propeller so much. Moreover, the maximum thrust of propeller mode is 22.5% higher than the water-jet mode and the maximum thrust of the hybrid mode is 2.27 times than the water-jet mode and 1.81 times than the propeller mode. In addition, to verify the low noise of the water-jet thruster, a noise comparison experiment is conducted and the results show that

the water-jet thruster has the low noise performance. Finally, in order to evaluate the performance of the SUR IV, some experiments in 3 DoF which include high-speed forward motion, dive and float motion, and rotation motion were completed in the swimming pool. The experimental result displays that the linear speed of the hybrid propulsion mode is 33.3% higher than that of the SUR III.

## References

Bhattacharyya, S., Asada, H. (2016). Single jet impinging verticial motion analysis of an underwater robot in the vicinity of a submerged surface. In Proceedings of 2016 IEEE oceans conference, pp. 1–8.

Chen, Z., Yu, J., Zhang, A., & Zhang, F. (2016). Design and analysis of folding propulsion mechanism for hybrid-driven underwater gliders. *Ocean Engineering, 119,* 125–134.

Chocron, O., Prieur, U., & Pino, L. (2014). A validated feasibility prototype for AUV reconfigurable magnetic coupling thruster. *IEEE/ASME Transactions on Mechatronics, 19*(2), 642–650.

Claus, B., Bachmayer, R., Cooney, L. (2012). Analysis and Development of a buoyancy pitch based depth control algorithm for a hybrid underwater glider. In Proceedings of 2012 IEEE/OES autonomous underwater vehicles (AUV), pp. 1–6.

Dong, Y., Duan, X., Feng, S., & Shao, Z. (2012). Numerical simulation of the overall flow field for underwater vehicle with pump jet thruster. *Procedia Engineering, 31*(2012), 769–774.

Drap, P., Scaradozzi, D., Gambogi, P., Gauch, F. (2008). Underwater cartography for archaeology in the VENUS project. (pp. 485–491). GRAPP.

Drap, P., Seinturier, J., Scaradozzi, D., Gambogi, P., Long, L., Gauch, F. (2007). Photogrammetry for virtual exploration of underwater archeological sites. In Proceedings of the 21st international symposium, (p. 1e6). CIPA.

Gao, B., Guo, S., & Ye, X. (2011). Motion-control analysis of ICPF-actuated underwater biomimetic microrobots. *International Journal of Mechatronics and Automation, 1*(2), 79–89.

Gasparoto, H., Chocron, O., Benbouzid, M., Meirelles, P. (2017). Magnetic design and analysis of a radial reconfigurable magnetic coupling thruster for vectorial AUV propulsion. In 2017 industrial electronics society, IECON 2017-43rd annual conference of the IEEE, pp. 2876–2881.

Georgiades, C., German, A., Hogue, A., Liu, H., Prahacs, C., Ripsman, A., & Dudek, G. (2004). AQUA: an aquatic walking robot. In Proceedings of 2004 IEEE/RSJ international conference on intelligent robots and systems (IROS). 4, pp. 3525–3531.

Gu, S., & Guo, S. (2017). Performance evaluation of a novel propulsion system for the spherical underwater robot (SUR III). *Applied Science, 7*(11), 1–19.

Gu, S., Guo, S., & Yao, Y. (2017). A hybrid propulsion device for the spherical underwater robot (SUR III). In *Proceedings of 2017 IEEE international conference on mechatronics and automation* (pp. 387–392).

Hanff, H., Kloss, P., Wehbe, B., Kampmann, P., Kroffke, S., Sander, A., Firvida, M., Einem, M., Bode, J., Kirchner, F. (2017). AUVx—a novel miniaturized autonomous underwater vehicle. In Proceedings of 2017 IEEE oceans conference, pp. 1–10.

Li, Y., & Guo, S. (2016). Communication between spherical underwater robots based on the acoustic communication methods. In *Proceedings of 2016 IEEE international conference on mechatronics and automation* (pp. 403–408).

Li, M., Guo, S., Hirata, H., & Ishihara, H. (2016). A roller-skating/walking mode-based amphibious robot. *Robotics and Computer-Integrated Manufacturing, 44,* 17–29.

Li, Y., Guo, S., & Wang, Y. (2017). Design and characteristics evaluation of a novel spherical underwater robot. *Robotics and Autonomous Systems, 94,* 61–74.

Li, Y., Guo, S., & Yue, C. (2015). Preliminary concept of a novel spherical underwater robot. *International Journal of Mechatronics and Automation, 5*(1), 11–21.

Lin, X., & Guo, S. (2012). Development of a spherical underwater robot equipped with multiple vectored water-jet-based thrusters. *Journal of Intelligent and Robotic Systems, 67*(3), 307–321.

Lin, X., Guo, S., Yue, C., & Du, J. (2013). 3D modelling of a vectored water jet-based multi-propeller propulsion system for a spherical underwater robot. *International Journal of Advanced Robotic Systems, 10*(1), 1–8.

Lv, X., Zhou, Q., & Fang, B. (2014). Hydrodynamic performance of distributed pump-jet propulsion system for underwater vehicle. *Journal of Hydrodynamics, 26*(4), 523–530.

Mai C., Pedersen S., Hansen L., Jepsen K., Yang Z. (2016). Subsea infrastructure inspection: a review study. In Proceedings of 2016 IEEE international conference on underwater system technology: theory and applications (USYS), pp. 71–76.

Mazumdar, A., Fittery, A., Ubellacker, W., Asada, H. (2013), A ball-shaped underwater robot for direct inspection of nuclear reactor and other water-filled infrastructure. In Proceedings of 2013 IEEE international conference on robotics and automation, pp. 3415–3422.

Pan, Q., Guo, S., & Okada, T. (2011). A novel hybrid wireless microrobot. *International Journal of Mechatronics and Automation, 1*(1), 60–69.

Russell, B., Veerle, A., Timothy, P., Bramley, J., Douglas, P., Brian, J., et al. (2014). Autonomous underwater vehicles (AUVs): their past, present and future contributions to the advancement of marine geoscience. *Marine Geology, 352,* 451–468.

Salumäe, T., Raag, R., Rebane, J., Ernits, A., Toming, G., Ratas, M., Kruusmaa, M. (2014). Design principle of a biomimetic underwater robot U-CAT. In Proceedings of 2014 oceans-St. John's, (pp. 1–5). IEEE.

Scaradozzi, D., Palmieri, G., Costa, D., & Pinelli, A. (2017a). BCF swimming locomotion for autonomous underwater robots: a review and a novel solution to improve control and efficiency. *Ocean Engineering, 130,* 437–453.

Scaradozzi, D., Palmieri, G., Costa, D., Zingaretti, S., Panebianco, L., Ciuccoli, N., et al. (2017b). UNIVPM BRAVe: a hybrid propulsion underwater research vehicle. *International Journal of Automation Technology, 11*(3), 404–414.

Vega, E., Chocron, O., & Benbouzid, M. (2016). A flat design and a validated model for an AUV reconfigurable magnetic coupling thruster. *IEEE/ASME Transactions on Mechatronics, 21*(6), 2892–2901.

Yue, C., Guo, S., Li, M., Li, Y., Hirata, H., & Ishihara, H. (2015a). Mechatronic system and experiments of a spherical underwater robot: SUR-II. *Journal of Intelligent and Robotic Systems, 80*(2), 325–340.

Yue, C., Guo, S., & Shi, L. (2013). Hydrodynamic analysis of the spherical underwater robot SUR-II. *International Journal of Advanced Robotic Systems, 10*(247), 1–12.

Yue, C., Guo, S., & Shi, L. (2015b). Design and performance evaluation of a biomimetic microrobot for the father–son underwater intervention robotic system. *Microsystem Technologies, 22*(4), 831–840.

Zheng, L., Guo, S., & Gu, S. (2018). The communication and stability evaluation of amphibious spherical robots. *Microsystem Technologies, 24,* 1–12.

Zhou, P., Liu, T., Zhou, X., Mou, J., Zheng, S., Gu, Y., et al. (2017). Overview of progress in development of the bionic underwater propulsion system. *Journal of Biomimetics, Biomaterials and Biomedical Engineering, 32,* 9–19.

**Publisher's Note** Springer Nature remains neutral with regard to jurisdictional claims in published maps and institutional affiliations.

**Shuoxin Gu** received the B.S. degree at Changchun University of Science and Technology (CUST), China, in 2011 and received the M.S. degree at Jilin University (JLU), China, in 2015. Now, Miss. Gu is as a Ph.D. student in Intelligent Mechanical Systems Engineering, Kagawa University (KU), Japan. She has published 2 conference papers and 1 journal paper in recent years. Her current research interests are spherical underwater robotics; bio-inspired robotics.

**Shuxiang Guo** received his Ph.D. degree mechano-informatics and systems from Nagoya University, Nagoya, Japan, in 1995. He had been a Full Professor at the Department of Intelligent Mechanical System Engineering, Kagawa University, Takamatsu, Japan, since 2005. He is also the Chair Professor in Key Laboratory of Convergence Medical Engineering System and Healthcare Technology, Ministry of Industry and Information Technology, Beijing Institute of Technology, China. He has published about 470 refereed journal and conference papers. His current research interests include biomimetic underwater robots and medical robot

systems for minimal invasive surgery, micro catheter system, micro-pump, and smart material (SMA, IPMC) based on actuators.

**Liang Zheng** received the B.S. degree and the M.S. degree at Changchun University of Science and Technology (CUST), China, in 2006 and 2010, respectively. Now, Mr. Zheng is as a Ph.D. student in Intelligent Mechanical Systems Engineering, Kagawa University (KU), Japan. He has published 1 conference papers and 1 journal paper in recent years. His current research interests are amphibious spherical underwater robotics; bio-inspired robotics.